

## Electronic Supplementary Information (ESI) for Soft Matter

### Modeling of Band-3 Proteins Diffusion in the Normal and Defective Red Blood Cell Membrane

He Li<sup>a</sup>, Yihao Zhang<sup>b</sup>, Vi Ha<sup>b</sup>, and George Lykotrafitis<sup>bc</sup>

<sup>a</sup> Division of Applied Mathematics, Brown University, Providence, RI 02912, USA

<sup>b</sup> Department of Mechanical Engineering, University of Connecticut, Storrs, CT 06269, USA

<sup>c</sup> Department of Biomedical Engineering, University of Connecticut, Storrs, CT 06269, USA

#### 1. The red blood cell (RBC) membrane model

The membrane of the RBC consists of spectrin tetramers which are connected at actin junctional complexes forming a 2D six-fold symmetric triangular network anchored to the lipid bilayer. Spectrin is a tetramer formed by head-to-head association of two identical heterodimers. Each heterodimer consists of an  $\alpha$ -chain with 22 triple-helical segments and a  $\beta$ -chain with 17 triple-helical segments<sup>1,2</sup>. In the proposed model, the spectrin is represented by 39 spectrin particles (white particles in Fig.1) connected by unbreakable springs. Thus, the equilibrium distance between (diameter of ) the spectrin particles is  $r_{\text{eq}}^{\text{s-s}} = L_{\text{max}} / 39$ , where  $L_{\text{max}}$  is the contour length of the spectrin ( $\sim 200$  nm), and  $r_{\text{eq}}^{\text{s-s}} \cong 5$  nm. Three types of coarse-grain (CG) particles are introduced to represent the lipid bilayer and band-3 proteins (see Fig. 1). The blue color particles denote a cluster of lipid molecules. Their diameter of 5 nm is approximately equal to the thickness of the lipid bilayer. The black particles represent glycoprotein proteins with the same diameter as the lipid particles. The band-3 protein consists of two domains: (i) the cytoplasmic domain of band-3 with a dimension of  $7.5 \times 5.5 \times 4.5$  nm that contains the binding sites for the cytoskeletal proteins, and (ii) the membrane domain, with a dimension of  $6 \times 11 \times 8$  nm, whose main function is to mediate anion transport<sup>3,4</sup>. We represent the membrane domain of band-3 by a spherical CG particle with a radius of 5 nm. The volume of the particle is similar to the excluded volume of the membrane domain of a band-3. However, when band-3 proteins interact with the cytoskeleton, the effect of the cytoplasmic domain has to be taken into account and thus in this case the effective radius is considered approximately 12.5 nm.

#### 2. Potentials implemented in the RBC membrane model

In the applied membrane model, the spectrin particles are connected by unbreakable springs. The employed spring potential  $u_{\text{cy}}^{\text{s-s}}(r) = k_0 (r - r_{\text{eq}}^{\text{s-s}})^2 / 2$  is plotted as the green curve in Fig. S1 with the equilibrium distance between the spectrin particles to be  $r_{\text{eq}}^{\text{s-s}} \cong 5$  nm. The two ends of the spectrin chains are connected to the actin junctional complexes via the spring potential  $u_{\text{cy}}^{\text{a-s}}(r) = k_0 (r - r_{\text{eq}}^{\text{a-s}})^2 / 2$ , where the equilibrium distance between an actin and a spectrin particle is  $r_{\text{eq}}^{\text{a-s}} = 10$  nm. The potential is plotted as the black curve in Fig. S1. The spring constant  $k_0 = 57 \varepsilon / \sigma^2$  is chosen to be identical with the curvature of the employed Lennard-Jones potential  $u_{\text{LJ}}(r_{ij}) = 4\varepsilon \left[ \left( \sigma / r_{ij} \right)^{12} - \left( \sigma / r_{ij} \right)^6 \right] + \varepsilon$  at the equilibrium to reduce the number of free parameters.

All spectrin particles interact with each other via the repulsive part of the L-J potential (Eq (1)). The lipid, glycoprotein, and band-3 CG particles carry both translational and rotational degrees of freedom ( $\mathbf{x}_i, \mathbf{n}_i$ ), where  $\mathbf{x}_i$  and  $\mathbf{n}_i$  are the position and the orientation (direction vector) of particle  $i$ , respectively. The rotational degrees of freedom obey the normality condition  $|\mathbf{n}_i| = 1$ . Thus, each

particle effectively carries 5 degrees of freedom.  $\mathbf{x}_{ij} = \mathbf{x}_j - \mathbf{x}_i$  is defined as the distance vector between particles  $i$  and  $j$ .  $r_{ij} \equiv |\mathbf{x}_{ij}|$  and  $\hat{\mathbf{x}}_{ij} = \mathbf{x}_{ij}/r_{ij}$  are the distance and the unit vector respectively. The particles forming the lipid membrane and membrane proteins interact with one another via the pair-wise potential

$$u_{\text{mem}}(\mathbf{n}_i, \mathbf{n}_j, \mathbf{x}_{ij}) = u_R(r_{ij}) + A(\alpha, a(\mathbf{n}_i, \mathbf{n}_j, \mathbf{x}_{ij}))u_A(r_{ij}), \quad (\text{S.1})$$

where

$$\begin{cases} u_R(r_{ij}) = k\epsilon \left( \frac{R_{\text{cut,mem}} - r_{ij}}{R_{\text{cut,mem}} - r_{\text{eq}}} \right)^8 - k\epsilon & \text{for } r_{ij} < R_{\text{cut,mem}} \\ u_A(r_{ij}) = -2k\epsilon \left( \frac{R_{\text{cut,mem}} - r_{ij}}{R_{\text{cut,mem}} - r_{\text{eq}}} \right)^4 - k\epsilon & \text{for } r_{ij} < R_{\text{cut,mem}} \\ u_R(r_{ij}) = u_A(r_{ij}) = 0, & \text{for } r_{ij} \geq R_{\text{cut,mem}} \end{cases} \quad (\text{S.2})$$

$u_R(r_{ij})$  and  $u_A(r_{ij})$  are the repulsive and attractive components of the pair potential respectively, and  $\alpha$  is a tunable linear amplification factor. The function  $A(\alpha, a(\mathbf{n}_i, \mathbf{n}_j, \mathbf{x}_{ij})) = 1 + \alpha(a(\mathbf{n}_i, \mathbf{n}_j, \mathbf{x}_{ij}) - 1)$  tunes the energy well of the potential through which the fluid-like behavior of the membrane is regulated. In the simulations,  $\alpha$  is chosen to be 1.55 and the cutoff distance of the potential  $R_{\text{cut,mem}}$  is chosen to be  $2.6\sigma$ . The parameters  $\alpha$  and  $R_{\text{cut,mem}}$  are appropriately selected to maintain the fluid phase of the lipid bilayer.  $k$  is selected to be 1.2 for the interactions among the lipid particles and  $k = 2.8$  for interactions between the lipid and the protein particles, such as glycophorin and band-3. Detailed information about the selection of the potential parameters can be found in the authors' previous work<sup>5,6</sup>. Fig. S1 shows only the potential between lipid particles for  $A = 1$  (blue curve). The interactions between the cytoskeleton and the lipid bilayer are represented by the repulsive part of the L-J potential as shown in Fig. S1 (Black curve).

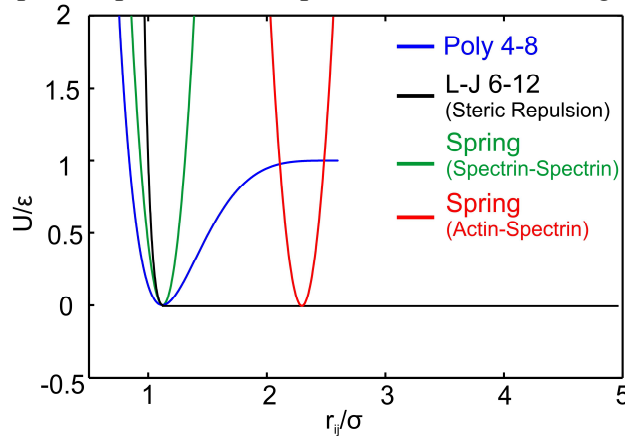


**Fig. S1** Interaction potentials used in the membrane model. The blue curve represents the potential between pairs of lipid particles. The green curve represents the spring potential between spectrin particles. The red curve represents the spring potential between actin and spectrin particles. The black curve represents the repulsive L-J potential between lipid and spectrin particles.

### 3. Persistence length corresponding to the spectrin filament model

To compute the persistence length  $l_p$  that corresponds to the introduced spectrin filament model we employed the expression  $\langle r_{ee}^2 \rangle^{1/2} \cong \sqrt{2l_p L_c}$ , where  $\langle r_{ee}^2 \rangle^{1/2}$  is the end-to-end distance of a thermally fluctuating flexible filament with a persistence length much smaller than its contour length  $L_c$  ( $l_p \ll L_c$ ). To calculate the end-to-end distance, we performed a molecular dynamics simulation of the spectrin chain model at the equilibrium temperature of  $T = 0.22\epsilon/K_B$ , where  $K_B$  is Boltzmann's constant. We first equilibrated the filament for  $10^5$  time steps and then measured the end-to-end distance for  $3 \times 10^6$  time steps. The measured values of  $\langle r_{ee}^2 \rangle^{1/2}$  follow a Gaussian distribution  $P(r_{ee}) = 1/(\lambda\sqrt{2\pi})\exp[-(r_{ee} - \langle r_{ee} \rangle)^2/2\lambda^2]$ , where  $\lambda = \sqrt{\langle (r_{ee} - \langle r_{ee} \rangle)^2 \rangle}$ , and with a mean value of  $\langle r_{ee}^2 \rangle^{1/2} = 75.4\text{nm}$  (Fig. S2). Considering that the spectrin contour length is approximately  $190\text{nm}$ <sup>7</sup>, we obtained a persistence length of approximately  $15\text{nm}$ . This result is close to the experimental values of approximately  $20\text{nm}$ <sup>8</sup> and  $10\text{nm}$ <sup>9</sup>.

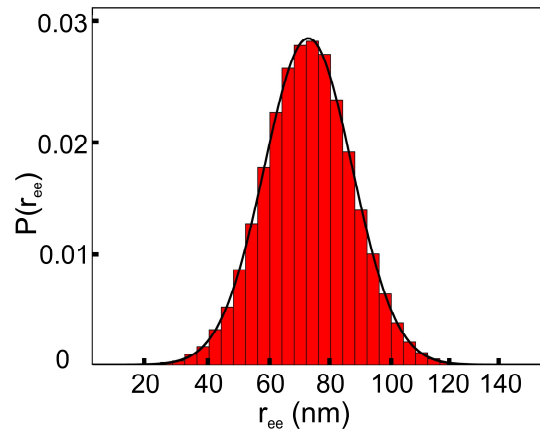


**Fig. S2.** Histogram of the recorded end-to-end distances ( $r_{ee}$ ) of a free spectrin filament during  $3 \times 10^6$  time steps of a coarse-grain solvent-free molecular dynamics simulation at constant temperature. The associated normalized Gaussian probability density (black line) is also shown.

### 4. Dependence of the diffusion coefficient of transmembrane proteins on their size

In the membrane model, the cytoskeleton of the RBC membrane acts as a barrier preventing band-3 proteins from crossing the spectrin filaments. Because the model is generic, we can easily consider the motion of other proteins of different sizes. This is especially interesting when the diffusive motion of adhesion receptors is explored. It is expected that large size proteins

compared to the average distance between spectrin filaments and the corresponding lipid bilayer are more likely to be hindered by the spectrin filaments leading to low diffusion coefficients. In contrast, the probability for smaller size proteins to cross the boundaries of the compartments is higher, resulting in larger diffusion coefficients. Here, we test the dependence of the diffusion coefficient on the size of the diffusing proteins in the lipid bilayer. In the manuscript, the domain of the membrane covered by a band-3 protein is considered to be a sphere of  $5nm$  radius while the effective cytosolic radius of the band-3 protein when it encounters a spectrin filament is selected to be  $12.5nm$  ( $2.8\sigma$ ). This accounts for the fact that band-3 proteins have a cylindrical overall structure protruding in the cytoplasm<sup>3,4</sup>. The corresponding macrodiffusion coefficient of band-3 particles moving in the RBC membrane with perfect spectrin network is  $D_{r_{\text{eff}}=2.8\sigma} = 1.95 \times 10^{-4} \sigma^2 / t_s$ . Next, we keep the membrane domain of protein particles the same as with the band-3 particles at  $5nm$  and we modify the effective radius. When the effective radius of the protein particle is increased to  $13.35nm$  ( $3.0\sigma$ ), the diffusion coefficient is decreased to  $D_{r_{\text{eff}}=3.0\sigma} = 0.83 \times 10^{-4} \sigma^2 / t_s$ , as shown in Fig S3. On the other hand, when the effective radius of the protein particles is decreased to  $11.8nm$  ( $2.65\sigma$ ) and  $10.9nm$  ( $2.45\sigma$ ) respectively, the diffusion coefficients increased to  $D_{r_{\text{eff}}=2.65\sigma} = 5.1 \times 10^{-4} \sigma^2 / t_s$  and  $D_{r_{\text{eff}}=2.45\sigma} = 9.7 \times 10^{-4} \sigma^2 / t_s$ . These measurements are consistent with our expectation and they illustrate the strong dependence of the diffusion coefficient on the endoplasmic size of transmembrane proteins.

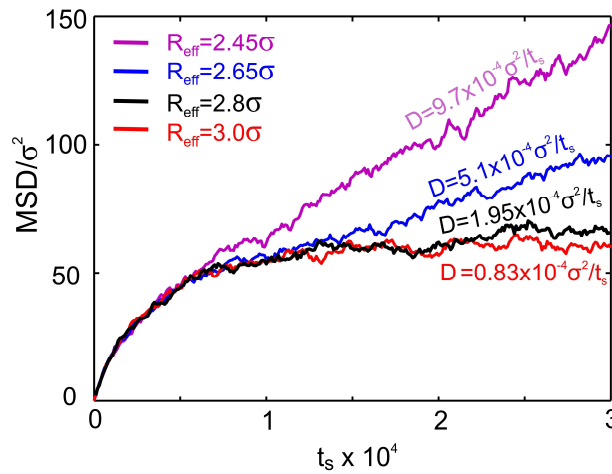


**Fig. S3** MSDs with respect to time and corresponding diffusion coefficients for mobile protein particles with different effective cytosolic radii as they diffuse in the RBC membrane with perfect cytoskeleton.

## 5. Additional Figures

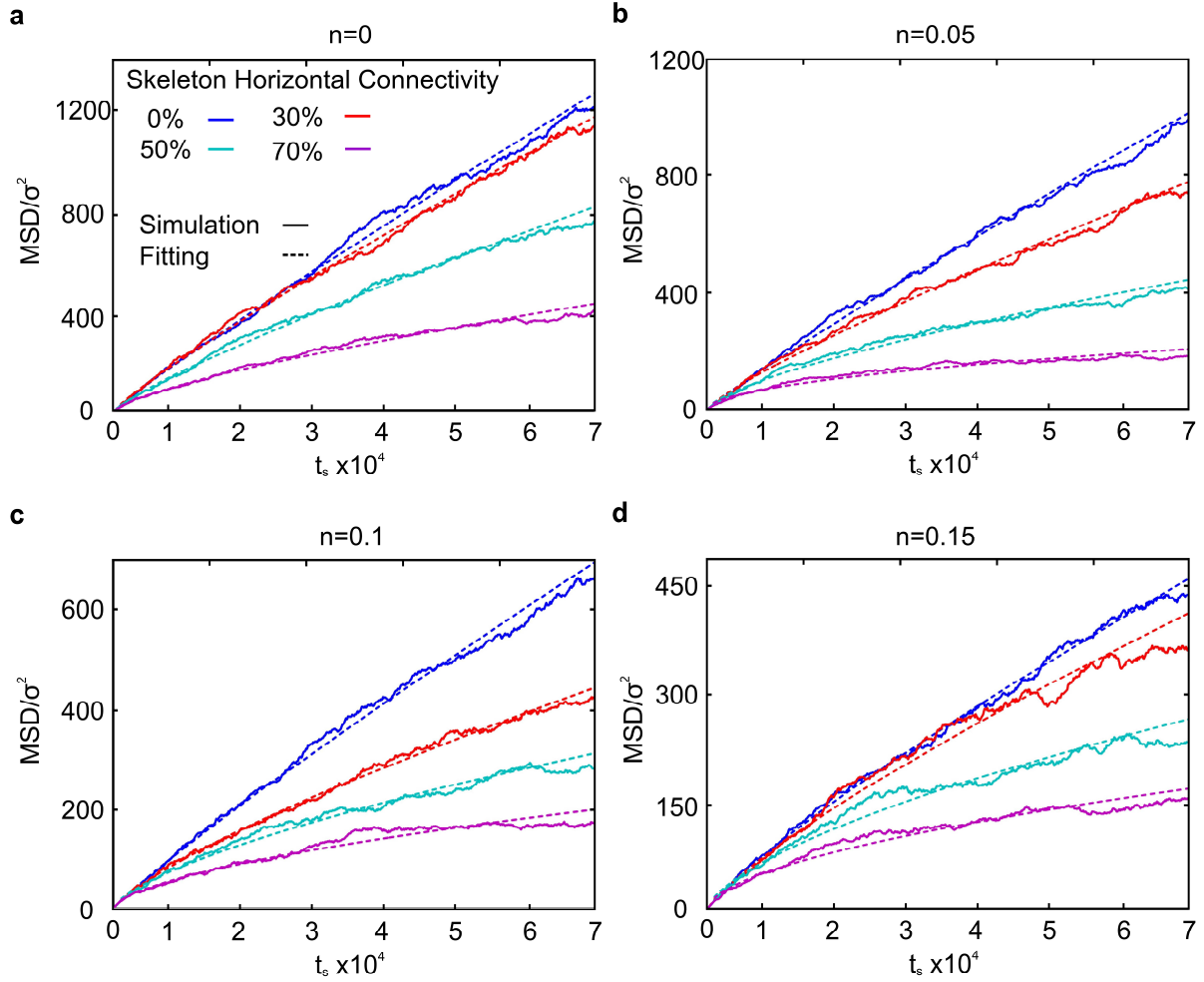


**Fig. S4** MSDs of band-3 particles with respect to time for different horizontal spectrin network connectivities. The dashed lines represent the power laws for the corresponding anomalous diffusion curves. The data are fitted from  $10^3 t_s$  until  $7 \times 10^4 t_s$ . The attraction levels between the lipid bilayer and the spectrin network have been adjusted to (a)  $n = 0$  (no attraction), (b)  $n=0.05$ , (c)  $n=0.1$ , and (d)  $n=0.15$ . The vertical connectivity is maintained at 100%.

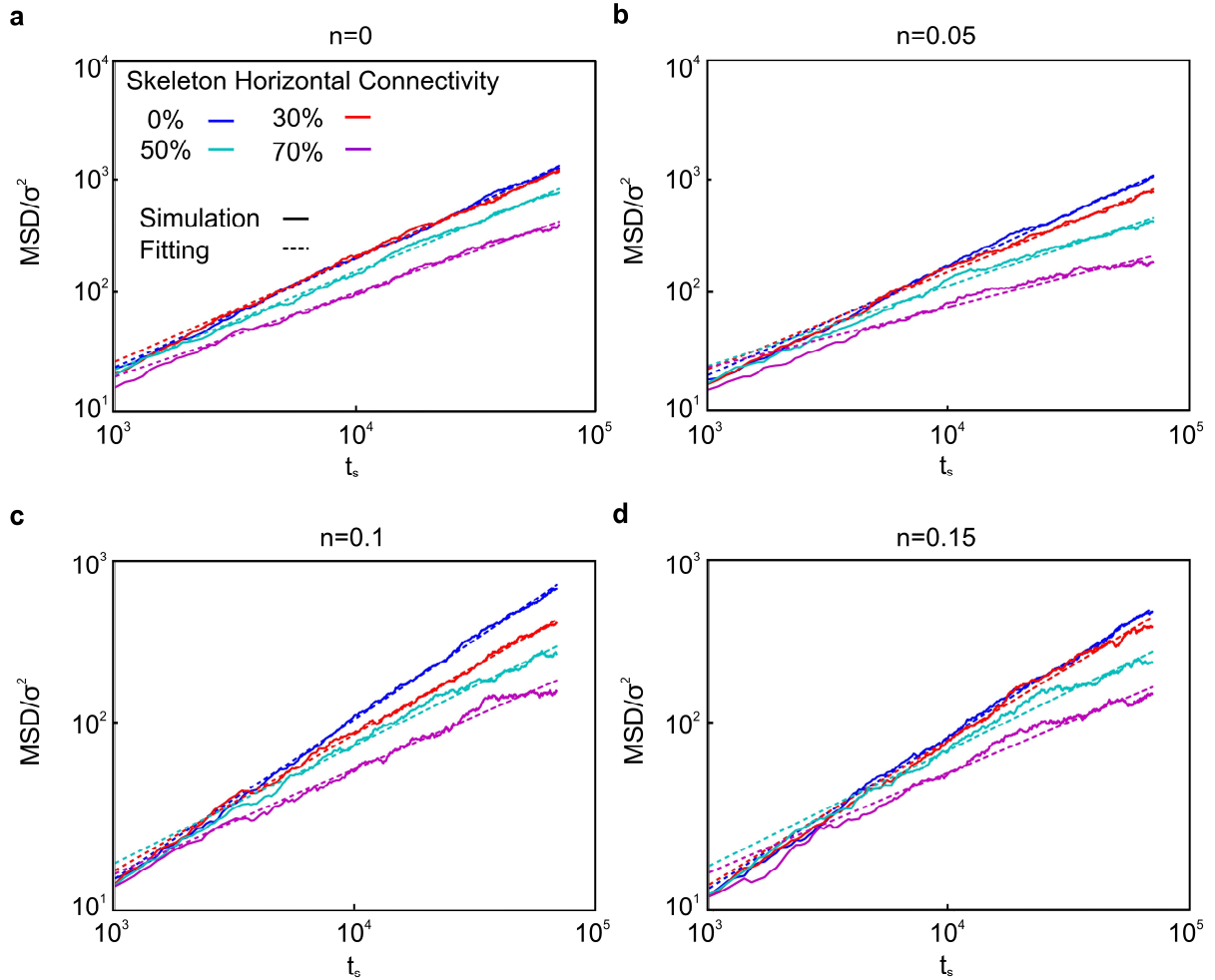


**Fig. S5** Logarithmic plot of the MSDs of band-3 particles with respect to time for different horizontal spectrin network connectivities. The dashed lines represent the power laws for the corresponding anomalous diffusion curves. The data are fitted from  $10^3 t_s$  until  $7 \times 10^4 t_s$ . The attraction levels between the lipid bilayer and the spectrin network have been adjusted to (a)  $n = 0$  (no attraction), (b)  $n=0.05$ , (c)  $n=0.1$ , and (d)  $n=0.15$ . The vertical connectivity is maintained at 100%.

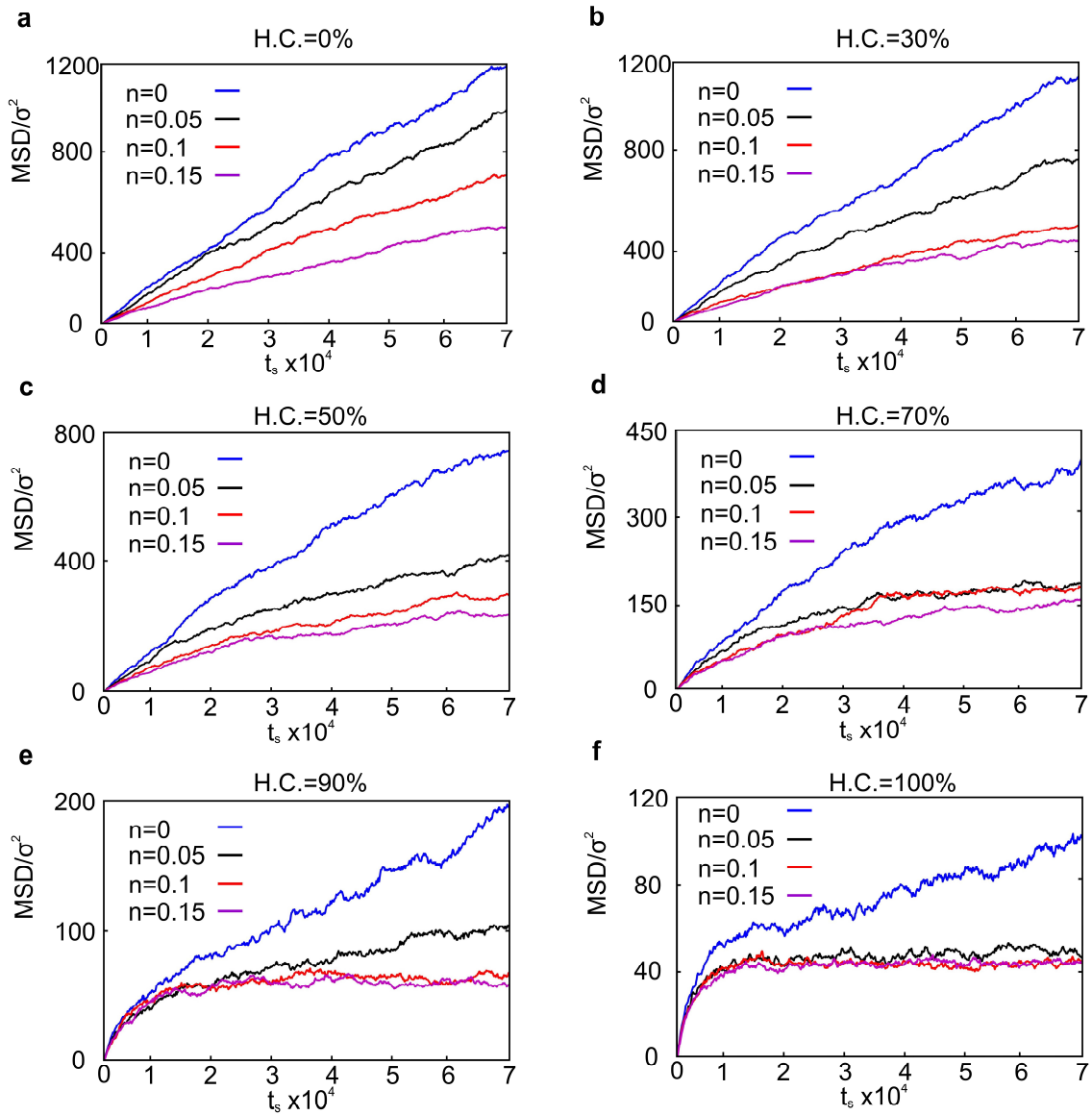


**Fig. S6** MSDs of band-3 particles with respect to time plots for different attraction levels between the lipid bilayer and the spectrin network. The horizontal spectrin network connectivities (H.C.) have been adjusted to (a) H.C. = 0%, (b) H.C.=30%, (c) H.C.=50%, (d) H.C.=70%, (e) H.C.=90%, and (f) H.C.=100%. The vertical connectivity is maintained at 100%.

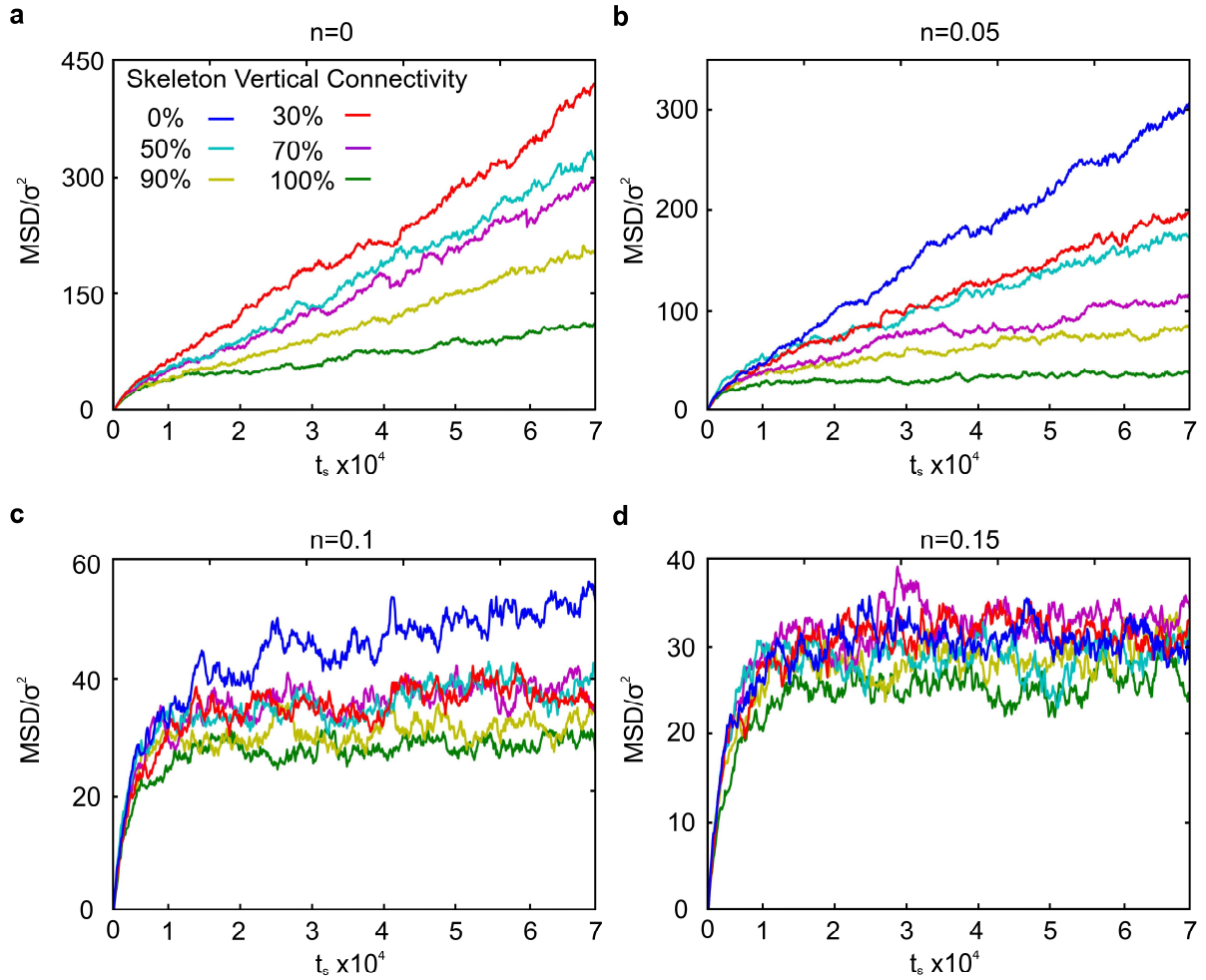


**Fig. S7** MSDs of band-3 particles with respect to time for different vertical connectivities between a perfect spectrin network and the lipid bilayer. The attraction levels between the lipid bilayer and the spectrin network have been adjusted to (a)  $n = 0$  (no attraction), (b)  $n=0.05$ , (c)  $n=0.1$ , and (d)  $n=0.15$ . The horizontal connectivity is maintained at 100%.

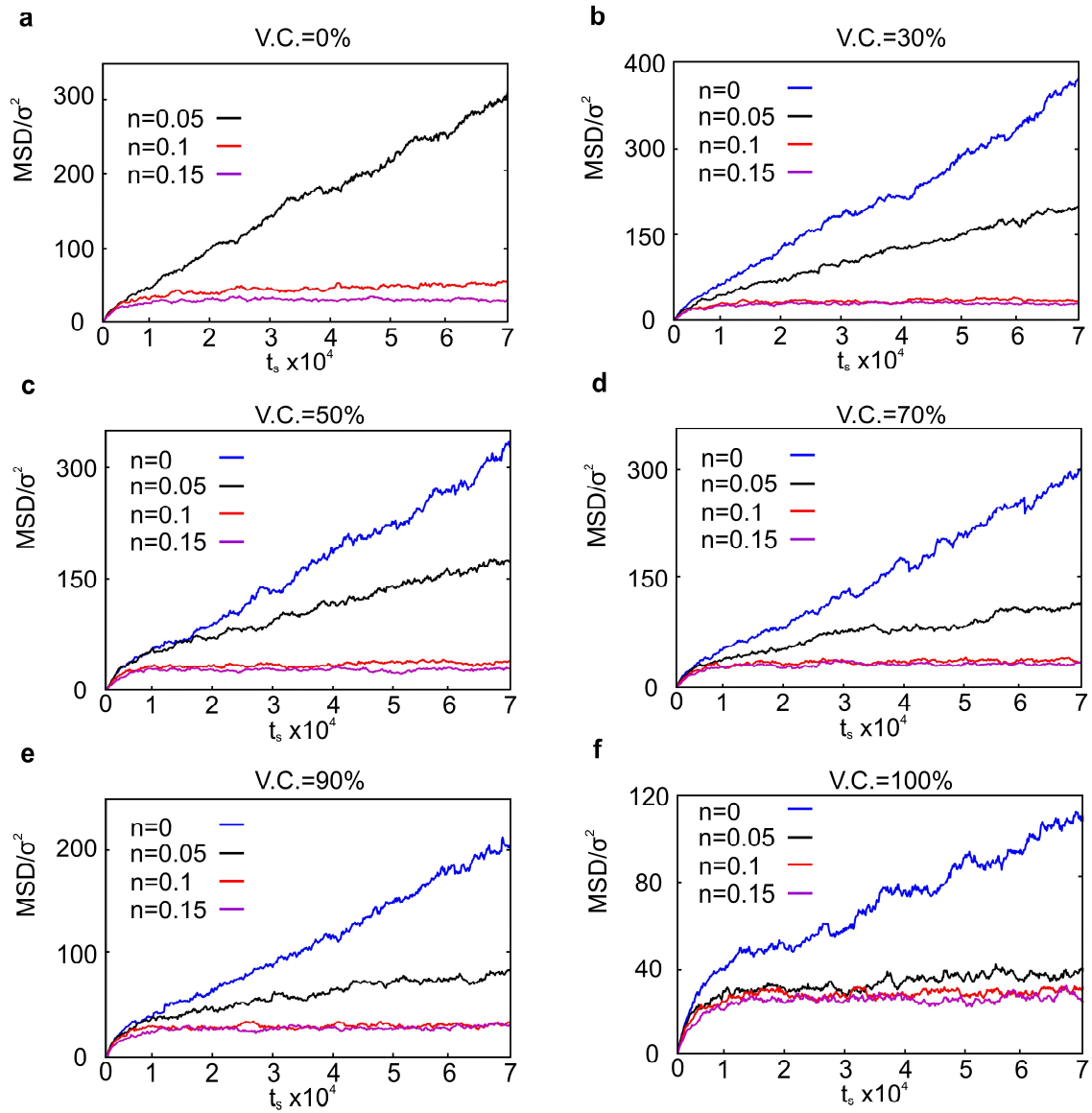


**Fig. S8** MSDs of band-3 particles with respect to time for different attraction levels between a perfect spectrin network and the lipid bilayer. The vertical connectivity (V.C.) between the cytoskeleton and the lipid bilayer has been adjusted to (a) V.C. = 0%, (b) V.C.=30%, (c) V.C.=50%, (d) V.C.=70%, (e) V.C.=90%, and (f) V.C.=100%. The horizontal connectivity is maintained at 100%.

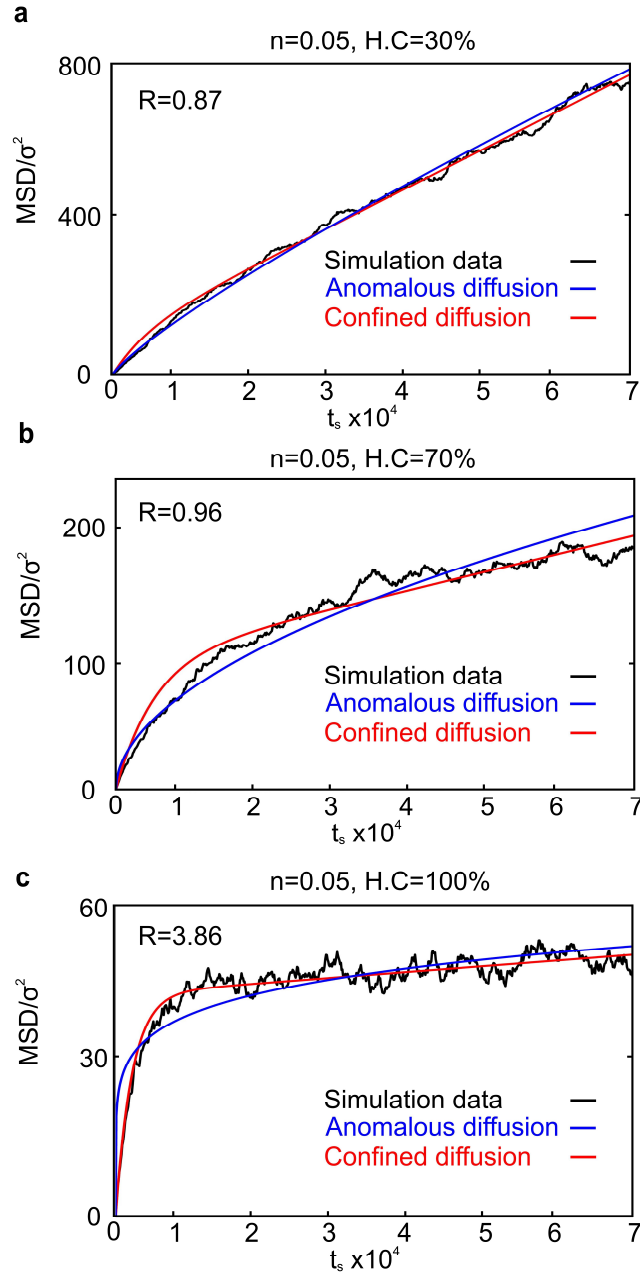


**Fig. S9.** The least squares approach is used to identify the parameters that best fit the numerical data (black curve) when anomalous diffusion (blue curve), for which  $MSD = At^\alpha$ , and confined diffusion (red curve), for which  $MSD(t) = 4D_{micro}\tau(1 - e^{-t/\tau}) + 4D_{macro}t$ , are considered.  $R$  represents the ratio of the sum of squares of residuals calculated for the anomalous diffusion over the confined diffusion. The confined diffusion fits the simulation results better for horizontal connectivities larger than 90%, while the anomalous diffusion is a better approximation for low horizontal connectivities.

## References

1. V. Bennett and A. J. Baines, *Physiol Rev*, 2001, **81**, 1353-1392.
2. B. Alberts, J. H. Wilson and T. Hunt, *Molecular biology of the cell*, Garland Science, New York, 2008.
3. D. N. Wang, V. E. Sarabia, R. A. Reithmeier and W. Kuhlbrandt, *EMBO J*, 1994, **13**, 3230-3235.
4. D. Zhang, A. Kiyatkin, J. T. Bolin and P. S. Low, *Blood*, 2000, **96**, 2925-2933.
5. H. Li and G. Lykotrafitis, *Biophysical Journal*, 2012, **102**, 75-84.
6. H. Li and G. Lykotrafitis, *Biophysical Journal*, 2014, **107**, 642-653.
7. D. M. Shotton, B. E. Burke and D. Branton, *J Mol Biol*, 1979, **131**, 303-329.
8. B. T. Stokke, A. Mikkelsen and A. Elgsaeter, *Biochim Biophys Acta*, 1985, **816**, 102-110.
9. K. Svoboda, C. F. Schmidt, D. Branton and S. M. Block, *Biophys J*, 1992, **63**, 784-793.